Geofísica Internacional (2020) 59-1: 39-53

Original paper

Distribution and current status of permafrost in the highest volcano in North America: Citlaltepetl (Pico de Orizaba), Mexico

Víctor Hugo Soto Molina and Hugo Delgado Granados

Received: August 30, 2018; accepted: December 09, 2019; published on line: January 06, 2020

Resumen

Se enfatiza la presencia de permafrost en el volcán Citlaltépetl y se actualiza su cubertura. Mediante el análisis empírico-estadístico de variables topo-climáticas y con base en el modelo de regresión lineal fue posible determinar que el límite inferior de permafrost continuo se ubica por encima de 4,880 msnm en la ladera norte y por arriba de 4,963 msnm en su ladera sur; por su parte, porciones discontinuas y aisladas inician a partir de 4,780 y 4,863 msnm al norte y sur del cono volcánico respectivamente. Se encontró una alta correlación entre la temperatura de los perfiles del suelo y la del aire en su altitud correspondiente. Las condiciones de temperatura del permafrost permiten considerarlo como "cálido", tal como sucede en montañas de mediana y baja latitud, y al mismo tiempo se puede clasificar como "comprometido" y potencialmente inestable. No obstante la degradación que presenta a partir de su primera estimación en los años 1970, se estima que este indicador de cambio climático de alta montaña permanezca al menos durante algunas décadas una vez que el glaciar del Citlaltépetl se haya extinguido.

Palabras clave: Permafrost, Citlaltépetl, Cambio climático, Temperatura del aire, Temperatura del suelo, Regresión lineal.

Abstract

The occurrence of permafrost in the Citlaltepetl volcano was emphasized and its coverage was updated. Through an empirical and statistical analysis of topo-climatic variables and based on linear regression it was found that the lower limit of continuous permafrost is positioned above 4,880 masl on its northern slope and at 4,963 on the southern slope; on the other hand, discontinuous and isolated patches start at 4,780 and 4,863 meters in the north and south respectively. A high correlation was found between the temperature of the ground profiles and the air temperature at their corresponding altitude. The temperature found in the permafrost classifies it as "warm" permafrost as in most mountains of medium and low latitude and at the same time it is classified as "compromised" and potentially unstable. In spite of the degradation observed from its first estimation during the 1970s, it is estimated that this indicator of climatic change in high mountains will remain at least for a few decades after the Citlaltepetl´s glacier has been extinguished.

Keywords: Permafrost, Citlaltepetl, Climate Change, Air temperature, Ground temperature, Linear regression.

V. H. Soto Molina
H. Delgado Granados
Departamento de Vulcanología
Instituto de Geofísica
Universidad Nacional Autónoma de México
Ciudad Universitaria
Delegación Coyoacán, 04510
Ciudad de México, México
Corresponding author: islaveracruz@gmail.com

Introduction

Among the four components of the planet's cryosphere (Williams, 2012): floating ice, seasonal snow, glaciers and permafrost, the last three are present in the upper part of the highest Mexican volcanoes: Citlaltepetl, Popocatepetl and Iztaccihuatl [5,610, 5,500 and 5,220 masl respectively (INEGI, 2017)]. Throughout the world, the high mountain landscape is evolving in an accelerated manner as a consequence of climate change (Spehn et al., 2005, Ahumada *et al*., 2010). Of their permanent ice, glaciers have dramatically retreated (Delgado-Granados, 2007; Herrera and Ruiz, 2009) or have been extinct for the past decades, and permafrost (Williams and Smith, 2008) has been degraded in recent years; at the same time, the permanence of seasonal snow has been progressively reduced. This together has forced the periglacial environment to experience geomorphological changes of different magnitude (Ahumada *et al.,* 2010); from the increase in areas of gelifluction (Janke *et al*., 2011), to rock fall and landslide with catastrophic results (Etzelmüller, 2013). Several investigations (Gruber *et al.,* 2004, Huggel *et al*., 2010, Clague *et al*., 2012) document that in many cases the degradation of permafrost has been the main conditioning factor.

Permafrost is a strictly thermal condition of the ground (French, 2007), and it is present in circumpolar regions as well as in some high mountain areas of medium and low latitude such as the Alps and the Andes especially; there are isolated mountains in regions of the tropics that also contain it. It is composed of rock or soil with or without the presence of organic elements in its interior that remain at least two continuous years below 0 ° C (Trombotto *et al.,* 2014); Above this is the active layer that is characterized by a cyclical freezing and thawing in response to the seasons of the year (Osterkamp and Jorgenson, 2009). Due to the physical-chemical characteristics of the soil and external processes such as the infiltration of water by melting and precipitation, the ice inside it may be present although it is not strictly necessary (French, 2007). To indicate the general characteristics of its coverage it is designated as "continuous permafrost" when it is present in more than 90% of the surface of the land; "discontinuous permafrost" is between 65 and 90% and "sporadic" below 65% (Trombotto *et al*., 2014).

Unlike the near-polar regions, the heterogeneity of the high mountain relief establishes the existence of microclimates among relatively small areas (Haeberli *et al.,* 2010) that often condition that air temperature and the correspondence with the presence of permafrost may differ substantially from the air-ground correlation present in circumpolar areas (Guodong and Dramis, 1992). While in Canada and Alaska the lower limit of continuous permafrost generally corresponds to an annual average air temperature (AAAT) of -6°C (Smith and Riseborough, 2002) and the discontinuous permafrost limit coincides with the annual isotherm of -1°C (Brown, 1970; French and Slaymaker, 1993), in mountains of medium and low latitude many times the presence of permafrost can occur with a AAAT above 0°C (Guodon and Dramis, 1992); such is the case of the Sierra de Telera, Spain (Andrés y Cía, 2006) and the Mauna Kea volcano, Hawaii with a AAAT of + 3.6°C (Woodcock, 1974, Gorbunov, 1978).

The periglacial environment in Mexico and particularly the topic of permafrost was addressed in glaciological studies at the end of the 1960s (Lorenzo, 1969a, Lorenzo, 1969b) and even more so during the 1970s through the studies of Heine (1973, 1975a, 1975b). , 1977), as well as Gorbonov (1978). Specifically, Heine (1975) performs a periglacial inventory on the Citlaltepetl volcano based on strictly visual descriptions, noting, in addition to other geomorphological features, that the lower limit of permafrost is located at 4,600 meters above sea level (masl). Again in the 1990s Heine (1994) reiterates the discontinuous presence of permafrost in the high Mexican mountains above the 4,600 level. During the last twenty years, most systematic works for the determination of permafrost in the country have begun, considering the thermal variable of the ground. These more recent researches have been carried out in the Popocatepetl and Iztaccihuatl volcanoes exclusively (Palacios et al., 2007, Andrés *et al.,* 2010, 2011, 2012), leaving aside the Citlaltepetl volcano, the highest in the country and in North America.

In the light of the above, this work has a dual purpose: in the first instance it aims to complement the most recent studies on permafrost in the three highest mountains in Mexico and secondly, it seeks to indicate the current state of its coverage in Citlaltepetl, which, in view of the current climate change conditions should be different from the one pointed out 43 years ago. The investigation is approached by analyzing the temperatures of ground profiles at different depths and their correlation with the AAAT; the degree of incidence of solar radiation on the surface and the albedo indexes are analyzed so that together the presence and limits of permafrost are indicated. The permanent existence of ice in the subsoil and rock confirms the above.

Geographic generalities of the study area

The volcano Citlaltepetl (Star hill in Nahuatl) or Pico de Orizaba is a stratovolcano that belongs to the Neo Volcanic Axis of Mexico in its easternmost area. The center of its crater is located at coordinates 97 ° 16' N and 19 ° 02' E (Rossotti *et al*., 2006). It has an altitude of 5,610 masl (INEGI, 2017) which makes it the highest volcano in North America and the third largest mountain after Mount Denali (6,190 masl) and Mount Logan (5,959 masl). Its age is dated in ~ 650,000 years when the first stage of formation known as "Torrecillas" began, which was followed by two more phases of evolution including "El Espolón de Oro" and the current crater (Macias, 2005). The most recent geological formations are a consequence of this last eruptive phase between 16,500 and 4,000 years ago (Macías, 2007); these are generally composed of dacite and andesite flows that cover large extensions of the north of the cone, some parts have been buried by deposits of pyroclastic material and ash; many of these materials have been compacted and others have a looser consistency (Carrasco-Núñez and Rose, 1995). The southern slope presents a significant flow of andesite from the same period and is mostly covered by pumice deposits that cover a large part of this slope with a gray-white color. The eastern and western slopes have lower amounts of lava flows that combine with deposits of pumice and ash. Above 4,000 masl the gelifraction process of the rock is noticeable, which in some cases forms conical deposits that flow according to the slope. The volcano has a clearly conical structure; the lava flows are located below the 4,900 level and above this limit its shape is markedly regular and homogeneous. On its north face and above 5,060 masl the glacier begins, extending continuously to the crater at the top of the cone; this summit divides the states of Puebla and Veracruz. In the slopes of the state of Puebla, the orography is very regular until it connects with the Central Mexican High Plateau with an average altitude of 2,200 masl; on the other hand, the relief is more rugged on the Veracruz side until it connects with the coastal plains of the Gulf of Mexico.

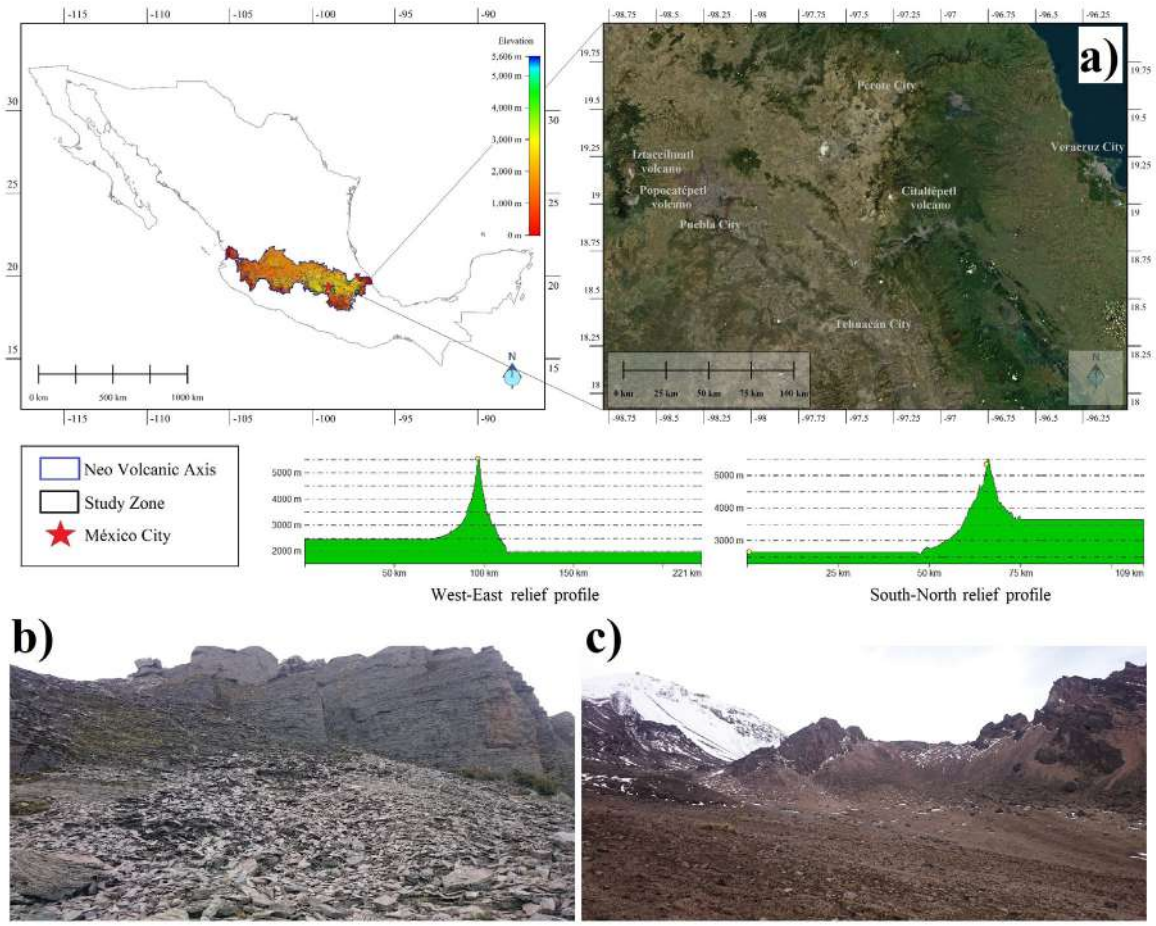

Figure 1. Study zone. Prepared by authors.

Materials and methods

To understand and indicate the presence of permafrost requires the combination of models and physical observations due to the systematic variability caused by the orography of the environment, which tends to be different from one area adjacent to another (Gruber and Haeberli, 2009). For this reason, in this work the current coverage of permafrost in the volcanic cone is evidenced and indicated through of a Geographic Information System (GIS) and under an empirical-statistical approach of topo-climatic variables [Julián and Chueca (2004), Julián and Chueca (2005), Abramov et al., (2008) and Serrano *et al*. (2009)].

Temperature

To confirm the presence of permafrost and to delimit its coverage under the thermal criteria, five observation stations were installed for the temperature of the sub-soil and air. Four of these stations were placed at different altitudes on the northern slope of the volcano and one more on the southern slope. To the north, the first one was installed at the timberline at 4,050 masl; the second at 4,200 masl, the third at 4,584 masl and the last near the lower limit of the glacier (5,060 masl). The southern station was placed under conditions similar to that of the northern elevation of 4,200, both in altitude and in the type of substrate and orographic conditions. At each station the ground was drilled to where the substrate and tools allowed under the PACE technical manual standards (Harris *et al.,* 2001) and the IPA (2008). In each perforation, a 2 "diameter PVC pipe was introduced, which was sealed at both ends; inside, Hobo Pendant UA-001-64 sensors were programmed and placed to log data every hour from March 22, 2015 until December 10, 2017. However, in order to avoid any uncertainty caused by considering incomplete years or seasons, the data analysis period for this work was two full years between July 1, 2015 and June 30, 2017. A sensor with the same characteristics was placed near each borehole to record the air temperature in equal periods. Figure 2 shows the position of the stations and the depths of each sensor.

Station	Longitude	Latitude	Altitude (masl)	Depth of sensors (cm)
1	-97°16'29.5''	19°04'20.8''	4,050	-5, -30, -60, -120
2	-97°16'23.9''	19°03'36.8''	4,200	-5, -40, -100, -175
3	-97°16'12.5''	19°02'46.7''	4,584	-5, -30, -60, -80
4	-97°16'10.6''	19°02'23.6''	5,060	-5, -50
5	-97°16'29.5''	19°00'18.2''	4,200	-5, -40, -100

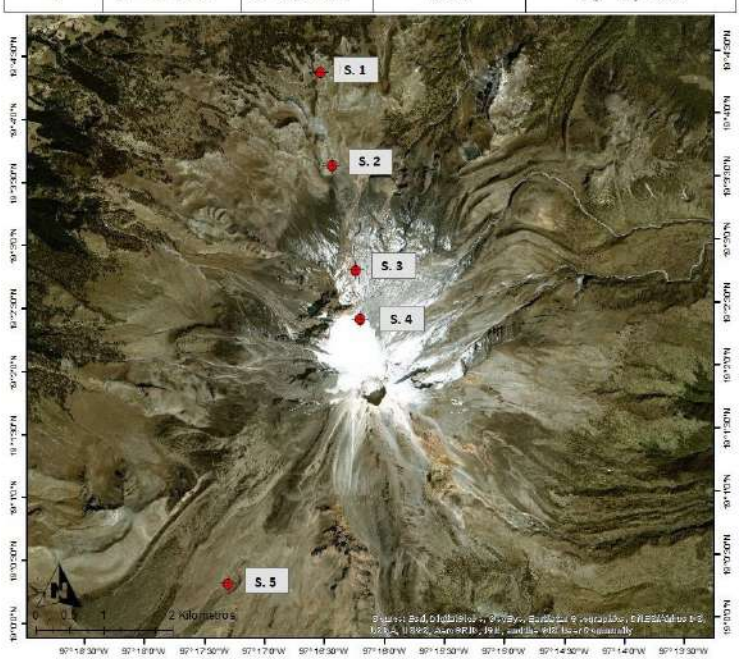

Figure 2. Location of the stations and depth of the sensors. Drilling at 5,060 masl was limited to only 50 cm due to the hardness of the frozen ground that was found. Prepared by authors.

The extraction and backup of the data was done every three months on average and during each visit the status of the batteries was tested; when they marked less than 50% of life they were replaced by new ones. The main objective of these tasks was to keep the sensors in optimal conditions for an uninterrupted temperature record and free of any alteration outside the characteristics of the weather that together would result in complete and homogeneous data series (Aguilar *et al*., 2003, OMM, 2011, Firat *et al.,* 2012).

The data of the two years were divided by month for each of the series and the monthly average was obtained, as well as the value of the annual average of both the air (AAAT) and the ground (AAGT) in the different depths to observe its oscillations throughout the year. In addition, monthly ground data were plotted along with their annual average value to analyze the temperature trend according to depth based on Williams and Smith (1989). At the same time the summer and winter periods were traced to further strengthen in the calculation of its temperature. Once the trend lines for the colder and warmer periods were joined at a point that manifested the absence of thermal oscillation between the two will mark the AAGT of each profile, and if this was within the range of negative temperatures would indicate the presence of permafrost (van Everdingen, 1985; French, 2007; Heginbottom *et al*., 2012). To determine the altitudinal limit of the permafrost, the equation of the regression line resulting from the correlation between the temperatures of the ground profiles and the altitude at which they are located was used; to ensure the quality of the estimation, statistical tests were performed on the residuals of the linear regression. Additionally, the AAAT records were used to compare with the AAGT of each profile; if the AAAT was negative at an altitude with a thermal profile that indicated the presence of permafrost, there would be an ideal air-ground correlation as suggested by Brown (1970), French and Slaymaker (1993) and Smith and Riseborough (2002). On the other hand, if the AAAT were higher than 0 ° C with a ground profile with permafrost, it would emphasize what was pointed out by Woodcock (1974), Gorbunov (1978), Guodong and Dramis (1992) and Andrés y Cía (2003).

Orography and incident solar radiation

In order to consider the different features of the relief, a digital terrain model (DTM) with a resolution of 2 meters per pixel was used. From this, the altitude as well as the aspect and slope characteristics were analyzed to determine the incident solar radiation (ISR). The ISR was calculated in ranges from low to high considering the values of the summer and winter solstices for a year through the Solar Radiation tool of ArcGis 10.4 which in turn is based on the algorithms of Fu and Rich (2000, 2002).

Albedo

It is widely documented that surface albedo greatly governs surface temperature when it comes to ISR (Liang *et al*., 2010). To observe the albedo index in the volcanic cone in ranges from 0 to 1 [considering that 0 represents a total absorption of incident solar energy and 1 is equivalent to the total reflection of that energy (Arya, 2001; Dobos, 2003)], a Landsat-5 satellite image with a resolution of 30 meters was used. Special care was taken to choose a cloud-free image over the study area and in a season totally free of seasonal snow. For this purpose, the image LT05_L1TP_025047_20091212_20161017_01_T1 was obtained from the USGS through the Earth Explorer platform. The surface albedo was obtained by the proposal of Liang (2000) and Liang *et al.* (2002) through the combination of bands 1, 3, 4, 5 and 7 by the equation:

$$\alpha = \frac{0.356_{p1}+0.130_{p3}+0.373_{p4}+0.085_{p5}+0.072_{p7}-0.0018}{0.356+0.130+0.373+0.085+0.072} \quad (1)$$

Where "α" is the albedo per pixel in the image, "p" is the band number and the values in thousandths correspond to the conversion factor for each of them. The processing was developed with the Map Algebra tool of ArcGis 10.4.

Once the presence of permafrost was determined directly by the temperature of the ground profiles and its altitude was delimited by linear regression, both the ISR and the albedo served to identify areas that despite being located tens of meters vertically below the limit lower of continuous permafrost, its low ISR range and a high albedo index, both in comparison to the values present in the zones previously identified through its temperature, allowed to consider them as areas of discontinuous permafrost that included isolated or sporadic patches. The visual recognition of ice in the subsoil (French, 2007) as interstitial or covered ice (Trombotto *et al.,* 2014) that remain throughout the year (Williams and Smith, 2008) and its georeferencing allowed to corroborate these areas. Finally the surface for each type was calculated with the Surface volume tool of ArcGis 10.4 considering the DTM to obtain the value of each area according to the altitude of the relief.

Results

The behavior of the monthly air temperature in each station shows an oscillatory pattern throughout the year that can be considered highly correlated (Motulsky and Christopoulos, 2003) in relation to the altitude at which they are located [Figure 3 (f)]. At 4,050 masl the range goes from 3.45 to 7.58°C and an AAAT of 4.97°C; at 4,200 masl, the thermal range is the lowest of all with values between 3.68 and 6.86°C and an annual average of 4.87°C. In level 4,584, the widest annual oscillation is recorded with values between -2.94 and 2.49°C with an average of 0.29°C. At 5,060 masl it varies from -2.99 to 1.06°C with an AAAT of -0.46°C. The southern station at 4,200 masl has a very similar oscillatory range, although slightly colder than its equivalent on the northern slope; their values range from 2.66 to 5.91°C with an annual average of 4.31°C. These patterns of behavior can be seen in Figure 3.

In the same way, the temperature profiles per altitudinal floor are shown in figure 4.

In ascending order of altitude, in the northern slope the temperatures found in the ground profiles are: at 4,050 masl, 7.80°C; at 4,200, 7.00°C; at 4,584 masl, 1.10°C and finally permafrost was located at elevation 5,060 with a temperature of -0.35°C. By using the regression equation of figure 4 (f) to determine the height at which the ground temperature is maintained at <= 0 ° C throughout the year, it is found that the lower limit of continuous permafrost is located at 4,880 masl. Figure 5 shows in summary the altitudinal estimate (shaded in black) and its statistical analysis.

A higher AAGT in the profile of the southern station is due to a greater amount of ISR [see figure 7 (a)]; it shows a value of 7.80°C at 4,200 masl. Considering the 0.80°C difference between the north and south profiles at 4,200 masl, it is assumed that the lower limit of the

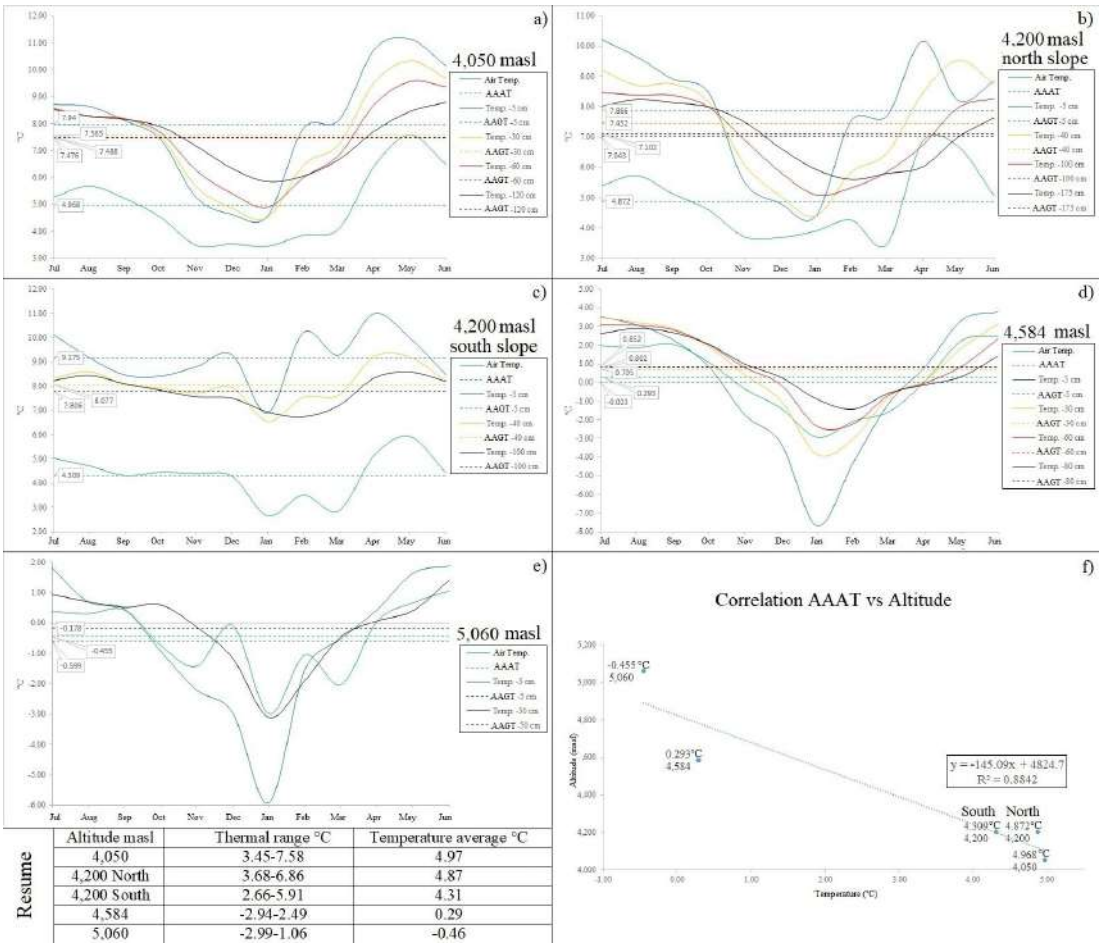

Resume

Altitude masl	Thermal range °C	Temperature average °C
4,050	3.45-7.58	4.97
4,200 North	3.68-6.86	4.87
4,200 South	2.66-5.91	4.31
4,584	-2.94-2.49	0.29
5,060	-2.99-1.06	-0.46

Figure 3. Monthly air and ground temperatures 2015-2017. The graph "f" indicates the correlation between the AAAT and the altitude of each station.

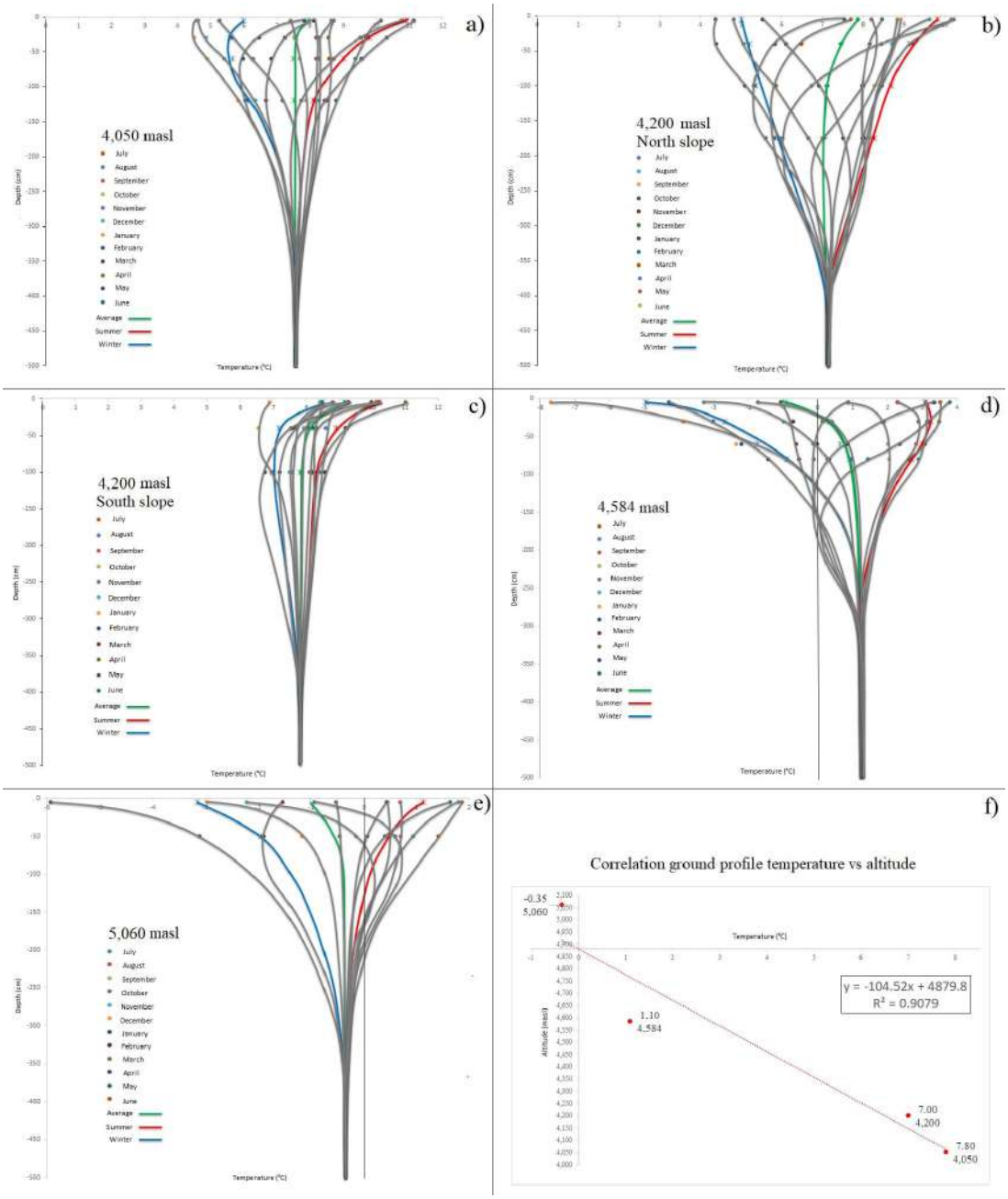

Figure 4. Monthly temperatures of the ground profiles 2015-2017. The graph "f" indicates the correlation with the altitude on the north slope. The crossing of axes "X" and "Y" is justified below.

continuous permafrost is located above the corresponding limit on the north side. In this way, if we use the previous regression equation once more to identify at what altitude the line crosses the -0.80°C we obtain as a result 4,963 masl as seen in figure 5. That is, while in the north the lower limit of continuous permafrost with a TMAS <= 0°C is located at 4,880 masl, in order to match that temperature in the south it would be necessary to ascend 83 meters more in vertical; so the permafrost cover, given the conical geometry of the volcano, would represent a concentric and at the same time elliptical shape (see figure 11). On the other hand, concerning the temperature of each profile and the value of the air temperature at the altitude at which they are located, there is an almost perfect correlation (Motulsky and Christopoulos, 2003) with R^2 = 0.99; this relationship is summarized in Figure 6.

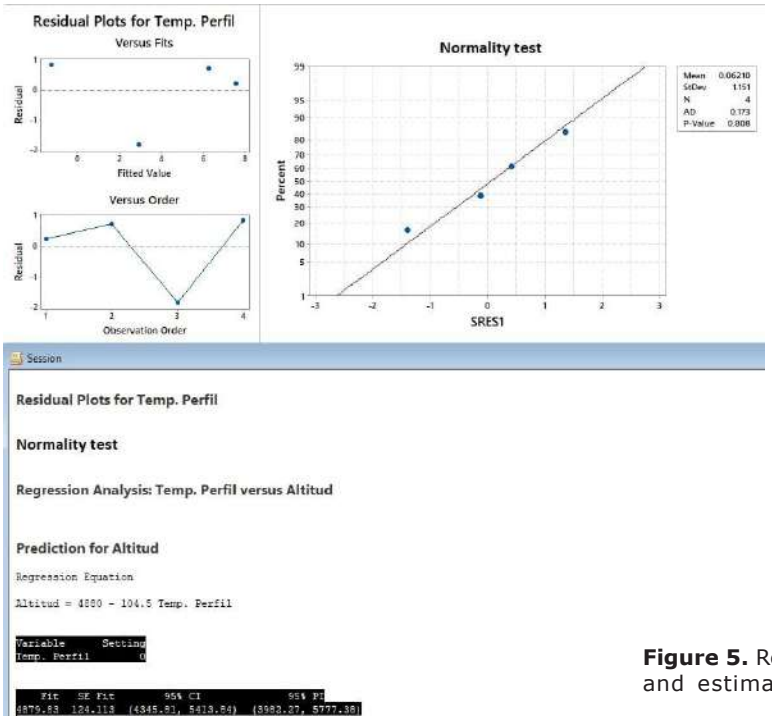

Figure 5. Regression analysis by means of residuals and estimation of the lower altitudinal limit of permafrost.

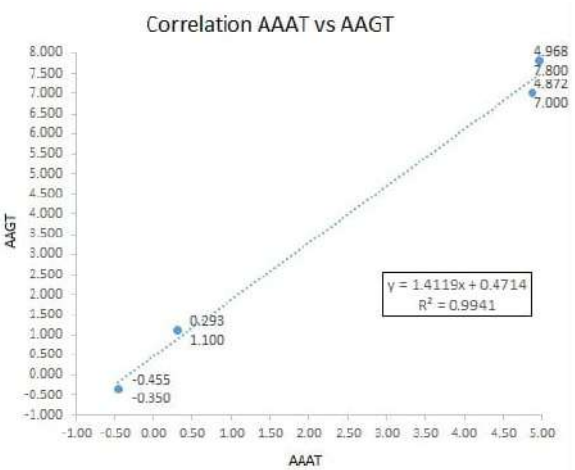

Figure 6. Air-ground correlation on the northern slope of the volcano. In this analysis, the southern slope station was not considered because, despite having an AAGT greater than that of its northern equivalent in response to a greater ISR, it has (as noted above) an AAAT 0.56°C lower.

Regarding the characteristics of the relief and its determining role on the ISR throughout the year, it can be seen in the map of figure 7 (a). In the same way, the particularities of reflection of the deposits determine the albedo indexes shown in the resulting map of Figure 7 (b).

The prospecting carried out along with the data mining allowed to identify large portions of ice buried by debris flows and deposits of finer materials above 4,700 masl. The location of these portions of buried ice suggest that they are remnants of the glacier which extended to this level during the year of 1975 (Cortés-Ramos and Delgado-Granados, 2015).

Additionally, ice outcrops are common through the rocky walls; many of these have remained throughout the time this work lasted, particularly those that are above 4,700 masl. The series of images shown in figure 9 provides an example of this.

There is also another type of geoform composed of detritus and cryoclasts with ice developed inside just below the set of nivodentritic channels at the foot of the remains of "El Espolón de Oro". The rich ice content in its interior could be the product of snow accumulation that has been covered by debris over time; it is suggested, according to Trombotto *et al.,* (2014) that it could represent a phase in the evolution of a debris glacier.

Therefore, it can be assumed that at least one hundred meters below the limit of continuous permafrost a parallel strip with a discontinuous and isolated presence of permafrost is located, which overall looks in accordance with figure 11.

Finally, the value of the areas of continuous and discontinuous permafrost cover, considering the orography, were estimated at 5.52 km^2 [this value does not consider the area of 0.61 km^2

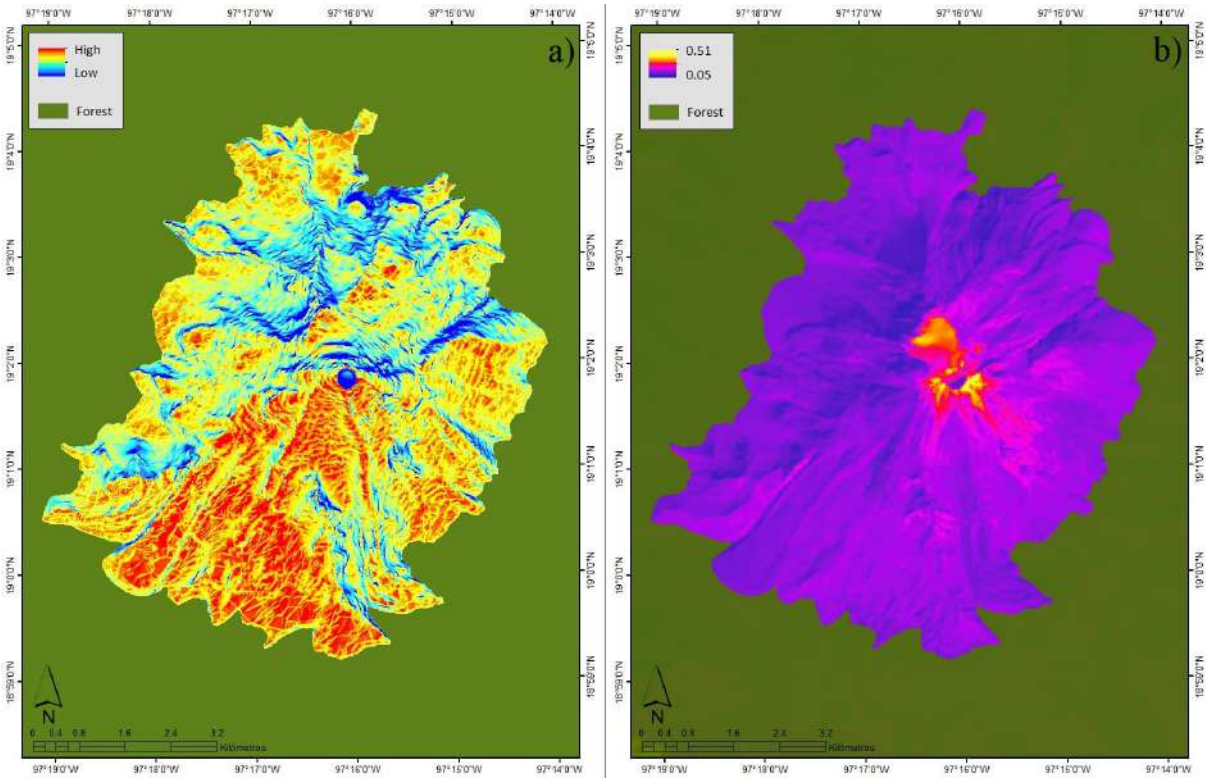

Figure 7. ISR (a) and albedo (b) maps. The highest albedo portion to the north of the crater belongs to the body of the glacier, while the rest are due to the reflectivity of the pumice deposits (Dobos, 2003, Ahrens, 2006). Prepared by authors.

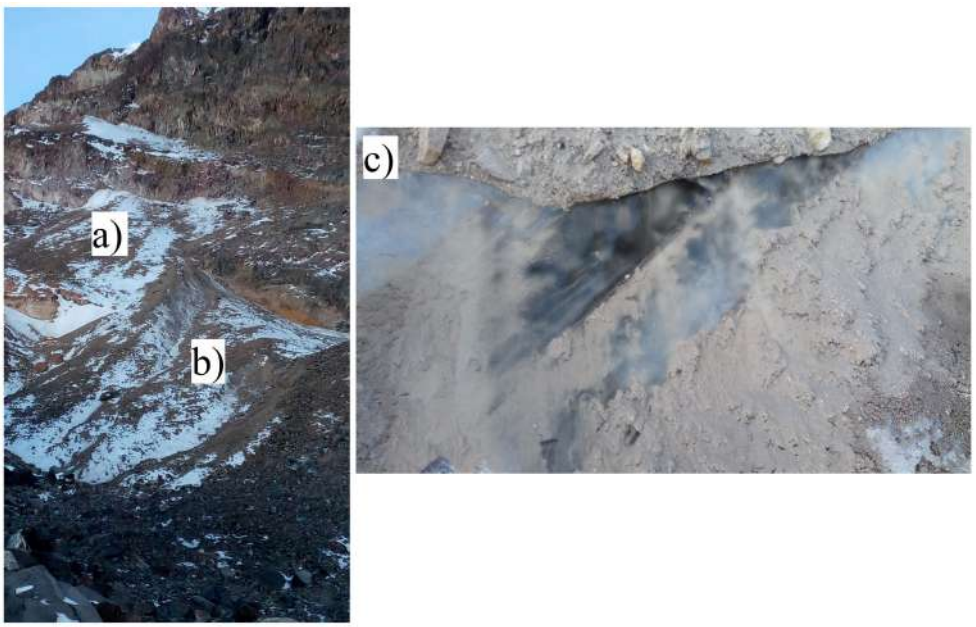

Figure 8. Buried ice in the northern slope. The image was taken at 4,810 masl, just below the "El Espolón de Oro"; it shows two isolated patches (a and b) of glacial ice buried by debris with a diameter of 2 to 12 cm. The linear section of exposed ice of patch b has a thickness of 60 cm and a length in the direction of the slope of approximately 65 meters. Photograph (c) shows in detail an exposed portion of solid ice below fine sediments and gravel.

Figure 9. Interstitial and intrusive ice. The sequence of previous photographs was taken at mid-day on May 31, 2016. The photo (a) was taken at 4,780 masl in the rocky portion known as "Los laberintos" and is visible through the cavities of the rock the lenticular ice agglomerations of 1 to 2 cm in diameter. Photo (b) shows a larger portion of ice that has formed in the middle of the separation of blocks of dacite from the flow of "Los laberintos" at 4,730 masl; it can be noticed the diagonally shaped 60 x 20 cm expanded between the spaces of the rock. The photograph (c) was taken close to 4,800 masl; the external part of approximately 90 x 40 cm of a solid portion of ice that covers the entrance of a rock cavity is clearly visible.

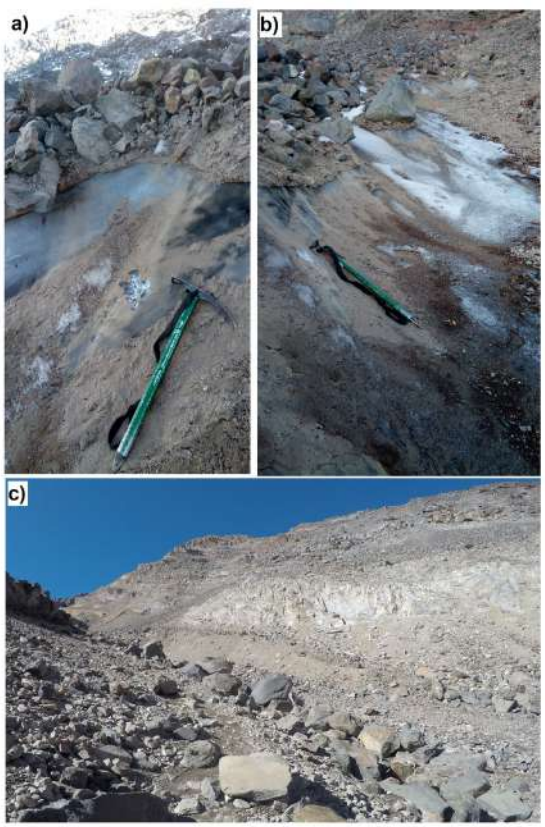

Figure 10. Protalus rampart on the northern slope. The photograph (a) shows the rich ice content by the recrystallization of the snow; in the background a part of the group of snow-debris channels can be seen. The exposed portion of massive ice shows a lobular shape that extends from the middle of the geoform to the upper part of it (photograph b). The photograph (c) was taken from an altitude of 4,700 masl; it exhibits the whole of the geoform that starts at 4.765 masl with an almost angular aspect close to the middle of its shape, product of the debris bearing above it that turn in the direction of the small valley downhill. In the background the summit of the "El Espolón de Oro" can be observed.

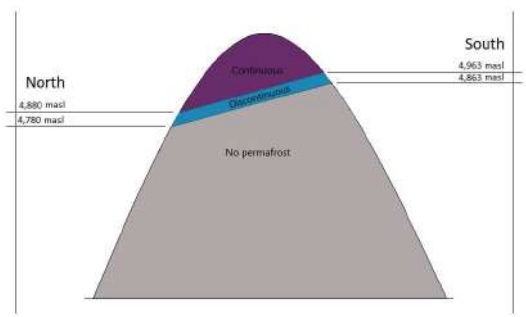

Figure 11. Schematic distribution of permafrost in the volcanic cone. The image has been made without considering scales. Prepared by authors.

(Cortés-Ramos, 2016) occupied by the glacier] and 2.06 km^2 respectively.

After the combination of variables, factors and elements analyzed in this paper, we can obtain the final map of permafrost distribution in the Citlaltepetl volcano (figure 12).

Discussion

After 43 years, when Heine (1975) pointed out the presence of permafrost in the volcano, it is still present in the Citlaltepetl. Although the author did not have prolonged temperature records to determine the permanence of the ground under freezing over at least two continuous years as is currently indicated in the specialized literature, this work confirmed its presence from the thermal perspective. The isolated and discontinuous portions that Heine found from 4,600 masl today are 180 meters above, an area we have identified as the discontinuous permafrost strip with an area of 2.06 km^2. On the other hand, the continuous permafrost cover is positioned at an average of 4,920 masl, considering the north and south slopes with an area of 5.52 km^2. The homogeneous characteristics of the relief and the material deposited above this level condition the continuous presence of permafrost.

The degradation of permafrost in the Citlaltepetl, although it is remarkable, has been presented more slowly compared to the retreat of its glacier. If we consider the northern slope where Heine (1975) indicates its beginning at 4,600 masl and that for that same year the lower limit of the glacier was calculated at 4,700 masl (Cortés-Ramos and Delgado-Granados, 2015), to compare it against our estimate of the discontinuous permafrost from 4,780 masl and currently at the beginning of the glacier at 5,060 masl, we obtain a retraction of 360 meters in the glacier against 180 meters of variation in the permafrost limit; in other words, the glacier has retreated at a rate of 8.6 meters per year compared to 4.3 meters per year of permafrost since 1975. These circumstances indicate the persistence of permafrost before the possible extinction of the glacier.

The large portions of ice found in the subsoil have remained at least for decades and are likely to remain even after the glacier has disappeared; on the other hand, the smaller fragments embedded in the rock walls may last only a few years due to the high rate of thermal conductivity offered by the rock (Vosteen and Schellschmidt, 2003).

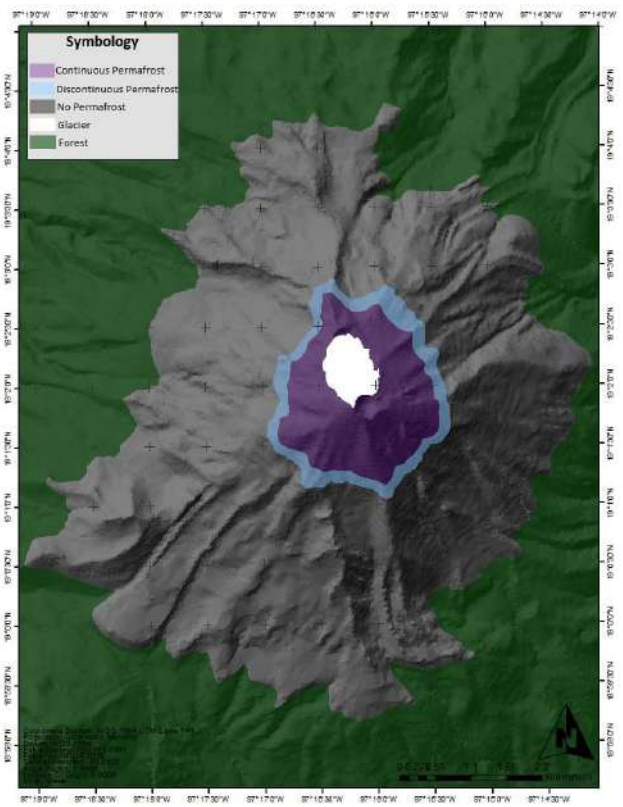

Figure 12. Map of distribution of permafrost in the Citlaltepetl volcano. Prepared by authors.

Although the surface of the south slope receives more ISR throughout the year compared to the north, its higher albedo index would balance its temperature to some extent. In spite of the fact that there is a warmer temperature of 0.56°C in the profile of the southern ground with respect to the north at 4,200 masl, the higher index of albedo above 4,800 masl compared to that of the northern slope at the same elevations and near the top it becomes equal or slightly higher than the one that presents the glacier ice of the north, it would come to "soften" the degree of ISR.

The regression model applied for the estimation of the lower limit of permafrost shows an acceptable level of certainty and is based on the high correlation existing (Motulsky and Christopoulos, 2003) between the AAGT of each profile and its corresponding altitude (R^2 = 0.91).

The AAAT and the AAGT in the north are perfectly matched (R^2 = 0.99). The case of the southern slope, at least for elevation 4,200 where the soil is warmer in response to the aforementioned ISR, the ground-air relationship deserves special attention and should be addressed in subsequent studies because its AAAT could be influenced for other micro-climatic factors.

The presence of permafrost in the station located at 5,060 masl and its corresponding value of air temperature (-0.35°C and -0.45°C respectively), as well as the AAGT-AAAT correlation indicated above indicate that at least for this mountain the permafrost interacts with an air temperature also below zero and at the same time make assume a balance between them.

The temperature conditions found in the permafrost classify it as "warm permafrost" (Noeztli *et al.,* 2003) and coincide very closely with those found by Andrés et al., (2010, 2011) and Yoshikawa (2013) in the tropical Chachani volcano (16 ° south latitude) of the Peruvian Andes and with the most of the high and low latitude permafrost in which its thermal conditions, always close to the thawing point, could allow them to be classified as "committed" and potentially unstable as suggested by Fischer et al., (2006).

Conclusions

The permafrost at Citlaltepetl is still present, but the degradation and retreat of its coverage is latent; this process is relatively similar to that of the retreat of its glacier in response to climate change as expressed by Wiliam and Smith (2008) and Ahumada et al., (2010). Notwithstanding the above, the rise of the lower limit of permafrost has been slower in comparison, as pointed out on a global scale by Fischer *et al.,* (2006) due to its hiding and protection characteristics provided by the surface and are contrary to direct exposure to the elements experienced by glacial ice. This suggests that of these two indicators of high mountain climate change, permafrost will remain at least a few decades after the glaciers are extinct.

This work updates the information provided in 1975 by Heine and complements the series of more systematic studies on permafrost coverage for the three highest mountains in the country.

Recommendations

Given its importance as an indicator of climate change, a continuous and uninterrupted monitoring of the permafrost temperature in the highest volcano in Mexico and North America, including, among other actions, the expansion of observation stations with records at a greater depth, is highly necessary in order to have a more complete and accurate database that serves as a basis for climate studies and subsequent geological risks.

References

Abramov, A., Gruber, S. and Gilichinsky, D., 2008. Mountain Permafrost on Active Volcanoes: Field Data and Statical Mapping, Klyuchevskaya Volcano Group, Kamchatka, Russia. *Permafrost and Periglacial Process*. Num. 19, pp. 261-277.

Aguilar, E., I. Auer, M. Brunet, et al., 2003. Guidelines on climate metadata and homogenization. WMO-TD No. 1186, WCDMP No. 53. WMO, 55.

Ahumada, A., Ibáñez, G., y Páez S., 2010. Reconocimiento de permafrost andino en las nacientes del río Santa María, Catamarca. *Ciencia*, Vol. 5 (13), pp. 95-110.

Andrés, A. J., & Cía, J. C., 2006. Modelización de la distribución del permafrost en la Sierra de Telera (Pirineo Central Español) a partir del empleo de Sistemas de Información Geográfica. *Rev. C & G.,* 20 (1-2): 25-46.

Andrés N., Zamorano, J., y Vázquez-Selem, L., 2010. Distribución del permafrost e intensidad de los procesos periglaciares en el estratovolcán Iztaccíhuatl (México). *Eria*, Num. 83, pp. 291-310.

Andrés, N., Palacios, D., Úbeda, J. and Alcalá, J., 2010. Ground thermal conditions at Chachani volcano, Southern Peru. *Geografiska Annaler: Series A, Physical Geography*, 93, 151–162. DOI: 10.1111/j.1468-0459.2011.00424.x

Andrés de Pablo, N. D., Estremera, D. P., Palenque, J. Ú., & Reygosa, J. A., 2011. Medio periglaciar, permafrost y riesgos naturales en un volcán tropical extinto: Nevado Chachani (sur de Perú). *Scripta Nova: revista electrónica de geografía y ciencias sociales*, (15), 376.

Andrés, N., Palacios, D., Zamorano, J. J., & Vázquez-Selem, L., 2011. Shallow ground temperatures and periglacial processes on Iztaccíhuatl volcano, Mexico. *Permafrost and Periglacial Processes*, *22*(2), 188-194.

Andrés, N., Palacios, D., Zamorano, J. J., Mendoza_Margain C., y Vázquez-Selem, L., 2012. "Temperatura del suelo en el volcán Popocatépetl: Implicaciones entre actividad volcánica y degladación". VIII Reunión Nacional de Geomorfología, Guadalajara, México.

Arya, P. S., 2001. *Introduction to micrometeorology* (Vol. 79). Academic press 420 pp.

Brown, R. J., 1970. *Permafrost in Canada: its influence on northern development*. University of Toronto Press.

Carrasco-Núñez, G., & Rose, W. I., 1995. Eruption of a major Holocene pyroclastic flow at Citlaltépetl volcano (Pico de Orizaba), México, 8.5–9.0 ka. *Journal of volcanology and geothermal research*, *69*(3), 197-215.

Clague, J. J., huggel, C., Korup, O., McGuire, B., 2012. Climate change and hazardous processes in high mountains. Revista de la Asociación Geológica Argentina, 69 (3): 328-338.

Cortés-Ramos, J., 2016. *Determinación de los regímenes glaciales en los volcanes Citlaltépetl e Iztaccíhuatl: factores físicos del retroceso y evolución glacial en México* (Doctoral thesis). Universidad Nacional Autónoma de México, Ciudad de México.

Cortés-Ramos, J., & Delgado-Granados, H., 2015. Reconstruction of glacier area on Citlaltépetl volcano, 1958 and implications for Mexico's deglaciation rates. *Geofísica internacional*, *54*(2), 111-125.

Delgado Granados, H., 2007. "Climate change vs. Volcanic Activity: Forcing Mexican Glaciers to Extinguish and Related Hazards. Proceedings of the First Internacional Conference on the Impact of Climate Change on High-Mountain Systems", Instituto de Hidrología, Meteorología y Estudios Ambientales, Bogotá, Colombia, pp. 153-168.

Dobos, E., 2003. Albedo, Encyclopedia of Soil Science. DOI: 10.1081/E-ESS 120014334.

Etzelmüller, B., 2013. Recent advances in mountain permafrost research. Permafrost and periglacial Processes, (24): 99-107.

Firat, M., Dikbas, F., Koc, A. C., & Gungor, M., 2012. Analysis of temperature series: estimation of missing data and homogeneity test. *Meteorological Applications*, *19*(4), 397-406.

Fischer, L., Kääb, A., Huggel, C., & Noetzli, J., 2006. Geology, glacier retreat and permafrost degradation as controlling factors of slope instabilities in a high-mountain rock wall: the Monte Rosa east face. *Natural Hazards and Earth System Sciences*, *6*(5), 761-772.

French H.M and Slaymaker O., 1993. Canada's cold land mass. In *Canada's Cold Environments*, French HM, Slaymaker O (eds). McGill-Queen's University Press: Montreal; 3–28.

French, H.M., 2007. The periglacial environment (3rd edition). Wiley and Sons, Chichester, 458 pp.

Fu, P., & Rich, P. M., 2000. The solar analyst 1.0 user manual. *Helios Environmental Modeling Institute*, *1616*.

Fu, P., & Rich, P. M., 2002. A geometric solar radiation model with applications in agriculture and forestry. *Computers and electronics in agriculture*, *37*(1-3), 25-35.

Gorbunov, A. P., 1978. Permafrost investigations in high-mountain regions. *Arctic and Alpine Research*, 283-294.

Gruber, S., Hoezle, M., Haeberli, W., 2004. Permafrost thaw and destabilization of Alpine rock walls in the hot summer of 2003. Geophysical research letters, vol. 31, L13504, doi: 10.1029/2004GL020051.

Gruber, S., y Haeberli, W., 2009. "Mountain permafrost" in R. Margesin (ed), *Permafrost Soils*, *Soil biology*, Springer-Verlag, Berlin.

Guodong, C., & Dramis, F., 1992. Distribution of mountain permafrost and climate.*Permafrost and Periglacial Processes*, *3*(2), 83-91.F

Haeberli, W., Noetzli, J., Arenson, L., Delaloye, R., Gärtner-Roer, I., Gruber, S., ... & Phillips, M., 2010. Mountain permafrost: development and challenges of a young research field. *Journal of Glaciology*, *56*(200), 1043-1058.

Harris, C., Haeberli, W., Vonder Mu¨ hll, D. & King, L., 2001. Permafrost monitoring in the high mountains of Europe: The PACE Project in its global context. Permafrost and Periglacial Processes 12, 3–11.

Heginbottom, A., Brown, J., Humlum, O., and Svensson, H., 2012. Permafrost and Periglacial Environments. *In* Williams Jr., Richard S. And Ferrigno, Jane (edts). State of the Earth´s Cryospherre at the Beginning of the 21st Century: Glaciers, Global Snow Cover, Floating Ice, and Permafrost and Periglacial Envoronments. U.S. Geologycal Survey Professional Paper 1386-A. 496 pp.

Heine, K., 1973. Variaciones más importantes del clima durante los últimos 40,000 años en México. *Comunicaciones,* Proyecto Puebla-Tlaxcala (Fundación Alemana de Investigaciones Científicas), 7: 51-58.

Heine, B., 1975a. Permafrost am Pico de Orizaba/Mexiko. *Eiszeitalter u. Gegenwart,* Vol 26, pp. 212-217.

Heine, K., 1975b. *Studien zur jungquartären Glazialmorphologie mexikanischer Vulkane: mit einem Ausblick auf die Klimaentwicklung* (Vol. 7). Steiner.

Heine, K., 1977. Zur morphologischen Bedeutung des Kammeises in der subnivalen Zone randtropischer semihumider Hochgebirge Beobachtungen aus Mexiko in den Jahren 1971-1975. *Z. Geomorph. NF*, *21*, 57-78.

Heine, K., 1994. Present and Past Geocryogenic Processes in Mexico. *Permafrost and Periglacial Processes,* Vol. 5(1): 1-12.

Herrera, G., y Ruiz, J., 2009. Retroceso glaciar en la Sierra Nevada del Cocuy, Boyacá-Colombia, 1986-2007. Perspectiva Geográfica. Vol. 13: 27-36.

Huggel, C., Fischer, L., Schneider, D., Haebeerli, W., 2010. Research advances on climate-induced slope instability in glacier and permafrost high-mountain environments. Geographica Helvetica (65): 146-156.

Instituto Nacional de Estadística, Geografía e Informática, INEGI, 2017. Anuario estadístico y geográfico de los Estados Unidos Mexicanos. INEGI c2017. Aguascalientes, Ags. 1066 pp.

International Permafrost Association, IPA, 2008. Manual for Monitoring and Reporting Permafrost Measurements, Part 1: Permafrost Borehole Temperatures and Part II Active Layer, draft. http://www.permafrostwatch.org/.

Janke, J. R., Williams, M. W., Evans Jr., A., 2011. A comparison of permafrost prediction models along a section of trail Ridge Road, Rocky Mountain National Park, Colorado, USA. Geomorphology. doi: 10.1016/j.geomorph.2011.08.029.

Julián, A., y Chueca, J., 2004. "El permafrost esporádico de la cara norte de la Sierra de Telera (Pirineo Aragonés)" en J.L. Peña, L.A. Longares y M. Sánchez (ed.), *Geografía Física de Aragón. Aspectos generales y temáticos.* Universidad de Zaragoza e Institución Fernando el Católico. Zaragoza, España.

Julián, A. y Chueca, J., 2005. Modelización de la distribución del permafrost en la Sierra de Telera (Pirineo central español) a partir del empleo de Sistemas de Información Geográfica en *Rev. C. and G.* Vol. 20, Núm. 1-2, pp. 25-46.

Liang, S., 2000. Narrowband to broadband conversions of land surface albedo algorithms. Remote Sensing of Environment 76, 213-238.

Liang, S., Shuey, C. J., Russ, A. L., Fang, H., Chen, M., Walthall, C. L., ... & Hunt Jr, R., 2002. Narrowband to broadband conversions of land surface albedo: II. Validation. *Remote Sensing of Environment*, *84*(1), 25-41.

Liang, S. L., K. C. Wang, X. T. Zhang, and M. Wild, 2010. Review on estimation of land surface radiation and energy budgets from ground measurement, remote sensing and model simulations, IEEE J. Sel. Top. Appl. Earth Obs. Remote Sens., 3(3), 225–240, doi:10.1109/ jstars.2010.2048556.

Lorenzo, J. L., 1969a. Condiciones periglaciares de las altas montañas de México, Instituto Nacional de Antropología e Historia. *Peleoelología*, 4: 1-45.

Lorenzo, J. L., 1969b. Minor periglacial phenomena among the high volcanoes of Mexico. *The periglacial environment: past and present*, 161-175.

Macías, J. L., 2005. Geología e historia eruptiva de algunos de los grandes volcanes activos de México. *Boletín de la Sociedad Geológica Mexicana*, *57*(3), 379-424.

Macías, J.L., 2007. Geology and eruptive history of some active volcanoes of México, in Alaniz-Álvarez, S.A., and Nieto-Samaniego, Á.F., eds., Geology of México: Celebrating the Centenary of the Geological Society of México: Geological Society of America Special Paper 422, p. 183–232, doi: 10.1130/2007.2422(06).

Motulsky, H. J., and Christopoulos, A., 2003. Fitting models to biological data using linear and nonlinear regression, A practical guide to curve fitting, GraphPad Software Inc., San Diego, CA. USA. 351 pp.

Noetzli, J., Hoelzle, M., & Haeberli, W., 2003. Mountain permafrost and recent Alpine rock-fall events: a GIS-based approach to determine critical factors. In *Proceedings of the 8th International Conference on Permafrost* (Vol. 2, pp. 827-832). Swets & Zeitlinger Lisse, Zürich.

Organización Meteorológica Mundial, OMM., 2011. Guía de prácticas climatológicas No. 100. ISBN 978-92-63-30100-0. Ginebra, Suiza. 128 pp.

Osterkamp, T. E., & Jorgenson, M. T., 2009. Permafrost conditions and processes. *Geological monitoring: Geological Society of America*, 205-227.

Palacios, D., Zamorano, J. and Andrés, N., 2007. "Permafrost Distribution in Tropical Stratovolcanoes: Popocatépetl and Iztaccíhuatl Volcanoes (Mexico)" in *Geophysical Research Abstracts*. Vol. 9, 05615.

Rossotti, A., Carrasco-Núñez, G., Rosi, M., & Di Muro, A., 2006. Eruptive dynamics of the "Citlaltépetl pumice" at Citlaltépetl volcano, eastern Mexico. *Journal of Volcanology and Geothermal Research*, *158*(3-4), 401-429.

Serrano, E., Morales, C., González-Trueba, J. y Martín, R., 2009. "Cartografía del permafrost de montaña en los pirineos españoles" en *Finisterra*. Vol. XLIV, Núm. 87, pp. 45-54.

Smith, M. W., & Riseborough, D. W., 2002. Climate and the limits of permafrost: a zonal analysis. *Permafrost and Periglacial Processes*, *13*(1), 1-15.

Spehn, Eva; Berge, Erling; Bugmann, Harald; Groombridge, Brian; Hamilton, Lawrence; Hofer,Thomas; Ives, Jack; Jodha, Narpat; Messerli, Bruno; Pratt, Jane; Price, Martin; Reasoner, Mel; Rodgers, Alan; Thonell, Jillian; Yoshino Masatoshi., 2005. Mountain Systems. *In* Hassan, Rashid; Scholes, Robert and Ash Neville (edts) Ecosystems and Human Well-being: Current State and Trends, Volume 1. Island press, Washington, DC. 901 pp.

Trombotto, D., Wainstein, P., Arenson, L., 2014. Guía Términológica de la Geocriología Sudamericana. Terminological Guide of the South American Geocryology.Vázquez Mazzini EditoresFundación de Historia Natural, Buenos Aires. 128 pp.

Van Everdingen, R.O., 1985. Unfrozen permafrost and other taliks, In: Brown, J., Metz, M. C. and Hoekstra, P. (eds), Proceedings of the Workshop on Permafrost Geophysics, US Army, CRREL, Special Report, 85-5, 101–105.

Vosteen, H. D., & Schellschmidt, R., 2003. Influence of temperature on thermal conductivity, thermal capacity and thermal diffusivity for different types of rock. *Physics and Chemistry of the Earth, Parts A/B/C*, *28*(9-11), 499-509.

Williams, Peter, J., and Smith Michael W., 2008.The frozen earth, Fundamentals of geocrynology. Cambrridge University Press. Cambridge, Uk. 323 pp.

Williams Jr., R. S., 2012. Changes in the earth´s cryosphere and global environmental change. *In* Williams Jr., Richard S. And Ferrigno, Jane (edts). State of the Earth´s Cryospherre at the Beginning of the 21st Century: Glaciers, Global Snow Cover, Floating Ice, and Permafrost and Periglacial Envoronments. U.S. Geologycal Survey Professional Paper 1386-A. 496 pp.

Woodcock, A. H., 1974. Permafrost and climatology of a Hawaii volcano crater. *Arct. Alp. Res*., 6(1): 49-62.

Yoshikawa, K. (ed.), 2013. *Permafrost in our time: community-based permafrost temperature archive*. University of Alaska Fairbanks Permafrost Outreach Program.